Bifurcation and chaos in high-frequency peak current mode Buck converter*

Chang-Yuan Chang(常昌远)†, Xin Zhao(赵欣), Fan Yang(杨帆), and Cheng-En Wu(吴承恩)

School of Integrated Circuit, Southeast University, Nanjing 210096, *China*

(Received 4 January 2016; revised manuscript received 17 March 2016; published online 31 May 2016)

Bifurcation and chaos in high-frequency peak current mode Buck converter working in continuous conduction mode (CCM) are studied in this paper. First of all, the two-dimensional discrete mapping model is established. Next, reference current at the period-doubling point and the border of inductor current are derived. Then, the bifurcation diagrams are drawn with the aid of MATLAB. Meanwhile, circuit simulations are executed with PSIM, and time domain waveforms as well as phase portraits in i_L–v_C plane are plotted with MATLAB on the basis of simulation data. After that, we construct the Jacobian matrix and analyze the stability of the system based on the roots of characteristic equations. Finally, the validity of theoretical analysis has been verified by circuit testing. The simulation and experimental results show that, with the increase of reference current I_{ref}, the corresponding switching frequency f is approaching to low-frequency stage continuously when the period-doubling bifurcation happens, leading to the converter tending to be unstable. With the increase of f, the corresponding I_{ref} decreases when the period-doubling bifurcation occurs, indicating the stable working range of the system becomes smaller.

Keywords: peak current mode Buck converter, high frequency, bifurcation, chaos

PACS: 05.45.–a, 84.30.Jc **DOI:** 10.1088/1674-1056/25/7/070504

1. Introduction

Switching DC–DC converters are strongly nonlinear systems with complex nonlinear phenomena, such as low-frequency oscillation,[1,2] period-doubling bifurcation, border collision bifurcation, chaos, and so on.[3–11] With the variation of circuit parameters, the converter systems may fall into chaotic state via various bifurcations, which have negative effects on their performance. Hence, it is of great importance to study nonlinear phenomena of the converters both in theory and application.

Nonlinear phenomena of DC–DC converters have been studied for many years. Previous literature mainly focus on peak current mode Boost converter[12–14] and current-mode Buck–Boost converter,[15–17] while research on peak current mode Buck converter started relatively late, and most of them employ an approximate one-dimensional discrete model, which fails to reflect the actual working situations of the converters.[3,18] Although there are some research studies that use a two-dimensional discrete model, their physical meanings are ambiguous.[19]

With the blooming development of science and technology, switching mode power supply develops rapidly in the direction of high frequency, miniaturization and light weight. Meanwhile, high-frequency switching power converters are widely applied in all kinds of portable electronic devices. Higher switching frequency means lower ripple of output voltage, thus reducing the required values of inductor and capacitor. Consequently, the sizes of passive devices can be reduced, making switching power converters smaller. However, most existing research is confined to low-frequency conditions (hundreds of kilohertz or lower).[20,21] Obviously, it is of great necessity to study those nonlinear phenomena in high-frequency switching power converters (switching frequency up to megahertz region), and to discover the relationship between switching frequency and system stability.

In this paper, the authors will study the nonlinear phenomena in high-frequency peak current mode Buck converter working in CCM. A precise two-dimensional discrete model is established in Section 2. In Section 3, the bifurcation diagrams of the system are plotted with the aid of MATLAB, meanwhile, circuit simulations are carried out with PSIM and the corresponding time domain waveforms as well as phase portraits in i_L–v_C plane are plotted with MATLAB. In addition, the critical reference current at the period-doubling point and the border of inductor current are derived in this part. In the following section, we derive the Jacobian matrix and analyze the stability of the system based on the roots of characteristic equations. Then in Section 5, an experimental circuit is built and tested to verify the validity of theoretical analysis. Section 6 gives the conclusion.

*Project supported by the National Natural Science Foundation of China (Grant No. 61376029), the Fundamental Research Funds for the Central Universities, China, and the College Graduate Research and Innovation Program of Jiangsu Province, China (Grant No. SJLX15_0092).

†Corresponding author. E-mail: ccyuan@163.com

© 2016 Chinese Physical Society and IOP Publishing Ltd

2. Dynamic modeling of peak current mode Buck converter

2.1. Working principle of peak current mode Buck converter

There exists a freewheeling diode which has significant forward voltage drop in a nonsynchronous Buck converter, thus reducing the efficiency of the system, and it is not in accord with the trend of low output voltage. As an alternative, the diode can be replaced by a low voltage drop power MOS transistor which is able to be easily embedded into a chip to achieve synchronous rectification, and the system efficiency can be improved accordingly.

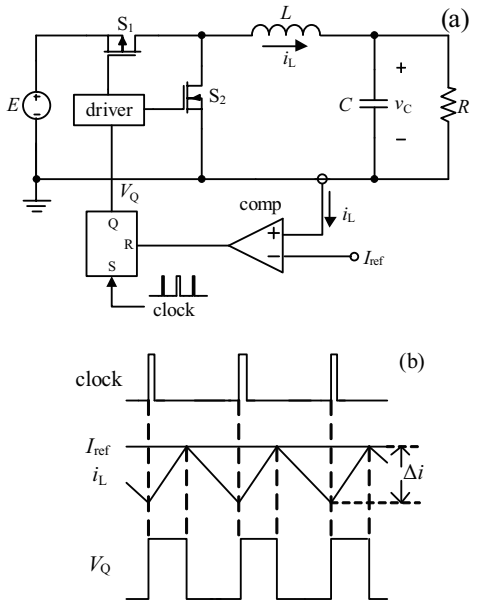


Fig. 1. (a) Schematic circuit diagram and (b) steady-state waveforms of peak current mode Buck converter.

Synchronous rectification technology is adopted in our design. The schematic circuit diagram of peak current mode Buck converter and its main working waveforms in steady-state are shown in Figs. 1(a) and 1(b), respectively.

When Buck converter works in CCM, the circuit will switch between two states. Using inductor current $i_{\rm L}$ and capacitor voltage $v_{\rm C}$ as state variables, we can obtain the dynamic equations of the system, which can be expressed as

$$\begin{cases} \dfrac{{\rm d}i_{\rm L}}{{\rm d}t} = -\dfrac{1}{L}v_{\rm C} + \delta\dfrac{1}{L}E, \\ \dfrac{{\rm d}v_{\rm C}}{{\rm d}t} = \dfrac{1}{C}i_{\rm L} - \dfrac{1}{RC}v_{\rm C}, \end{cases} \tag{1}$$

where E is the input voltage, $\delta = 1$ represents switch S_1 is on while $\delta = 0$ represents S_1 is off. Here, L, R, and C represent inductor value, resistor value, and capacitor value respectively.

It can be seen from Eq. (1) that the peak current mode Buck converter is a piecewise nonlinear dynamic system, and it is hard to analyze its dynamic behavior with the aid of dynamic equations directly, while utilizing discrete iterative mapping model will be a smarter choice.

2.2. Discrete iterative mapping model

Sampling state variables is needed when establishing the discrete iterative mapping model of peak current mode Buck converter. Based on various sampling methods, modeling approaches can be divided into the stroboscopic map, synchronous switching map and asynchronous switching map, among which the stroboscopic map is the most widely used method to study nonlinear phenomena in switching converters.[22] We utilize the stroboscopic map to build discrete iterative mapping model of peak current mode Buck converter, and using $i_n = i_{\rm L}(nT)$, $v_n = v_{\rm C}(nT)$ to represent the sampling values of inductor current and capacitor voltage at time nT respectively. Similarly, i_{n+1} and v_{n+1} represent the sampling values of inductor current and capacitor voltage at time $(n+1)T$ respectively. The switchover of the MOS tubes only occurs when $i_{\rm L} = I_{\rm ref}$.

MOS tube S_1 will be turned off if inductor current $i_{\rm L}$ increases to $I_{\rm ref}$. According to Eq. (1), we could calculate the rise time of inductor current during the switching cycle n, namely the conduction time t_n of switch tube S_1, which is

$$t_n = L\frac{I_{\rm ref} - i_n}{E - v_n}. \tag{2}$$

When $t_n \geq T$, switch tube S_1 is on during the entire switching cycle, and the corresponding discrete iterative mapping model of the converter can be expressed as follows:

$$i_{n+1} = {\rm e}^{\alpha T}(c_1\cos\beta T + c_2\sin\beta T) + \frac{E}{R}, \tag{3}$$

$$v_{n+1} = {\rm e}^{\alpha T}(c_3\cos\beta T + c_4\sin\beta T) + E, \tag{4}$$

where

$$\alpha = -\frac{1}{2RC}, \quad \beta = \sqrt{\frac{1}{LC} - \frac{1}{4R^2C^2}},$$
$$c_1 = i_n - \frac{E}{R}, \quad c_2 = \frac{1}{\beta}\left[\frac{E - v_n}{L} - \alpha\left(i_n - \frac{E}{R}\right)\right],$$
$$c_3 = v_n - E, \quad c_4 = \frac{\alpha}{\beta}(v_n + E) + \frac{i_n}{\beta C}.$$

When $t_n < T$, switch tube S_1 will be shut off after a period of time, resulting in the turn-off time in a switching cycle is $T - t_n$. Accordingly, we can derive the discrete iterative mapping model of the converter in this condition

$$i_{n+1} = {\rm e}^{\alpha(T-t_n)}\left(k_1\cos\beta(T-t_n) + k_2\sin\beta(T-t_n)\right), \tag{5}$$

$$v_{n+1} = -L{\rm e}^{\alpha(T-t_n)}\Big[(k_1\alpha + k_2\beta)\cos\beta(T-t_n) + (k_2\alpha - k_1\beta)\sin\beta(T-t_n)\Big], \tag{6}$$

where

$$k_1 = I_{\rm ref}, \quad k_2 = -\frac{1}{\beta L}\left(v_{\rm C}(0) + \alpha L I_{\rm ref}\right),$$
$$v_{\rm C}(0) = {\rm e}^{\alpha t_n}\left(c_3 \cos\beta t_n + c_4 \sin\beta t_n\right) + E.$$

Consequently, equations (3)–(6) form the accurate two-dimensional discrete iterative mapping model of the peak current mode Buck converter.

3. Analysis of dynamic behaviors in peak current mode Buck converter

3.1. The period-doubling bifurcation and border collision bifurcation

Many parameters of the DC–DC converters can be used to study nonlinear behaviors. However, in the following analysis, we only focus on the influence of reference current $I_{\rm ref}$ and switching frequency f.

For a peak current mode Buck converter, it is widely known that period-doubling bifurcation occurs when the duty cycle D exceeds 0.5.[3,4,18] According to Eq. (1), the peak–peak value of inductor current ripple can be calculated as

$$\Delta i = \frac{DT(E - v_{\rm C})}{L} = \frac{D(1-D)TE}{L}. \tag{7}$$

Based on the power-balance equation, we can obtain

$$E\left(I_{\rm ref} - \frac{\Delta i}{2}\right) = \frac{D^2E^2}{R}. \tag{8}$$

Combining Eq. (7) with Eq. (8) and substituting $D = 0.5$ into the new equation, we can obtain the critical reference current as the period-doubling bifurcation occurs, which is

$$I_{\rm ref,pdb} = \frac{E}{R}\left(\frac{TR}{8L} + \frac{1}{4}\right) = \frac{E}{R}\left(\frac{R}{8Lf} + \frac{1}{4}\right). \tag{9}$$

Besides, there exists a border of inductor current in the discrete iterative mapping model of peak current mode Buck converter working in CCM. We define $I_{\rm b}$ as the corresponding initial inductor current value at the beginning of a switching cycle provided that inductor current will exactly increase to reference current $I_{\rm ref}$ at the end of the switching cycle. By substituting $I_{\rm b}$, $I_{\rm ref}$ for i_n, i_{n+1} in Eq. (3) respectively, then the border $I_{\rm b}$ can be obtained as

$$I_{\rm b} = \frac{{\rm e}^{-\alpha T}\left(I_{\rm ref} - \frac{E}{R}\right) + \frac{E}{R}\cos\beta T - \frac{1}{\beta}\left(\frac{E - v_n}{L} + \frac{\alpha E}{R}\right)\sin\beta T}{\cos\beta T - \frac{\alpha}{\beta}\sin\beta T}. \tag{10}$$

Next, serve reference current $I_{\rm ref}$ as bifurcation parameter, and alter its value from 0.8 A to 1.5 A continuously. The system parameters are $E = 3.3$ V, $L = 4.7$ μH, $C = 10$ μF, $R = 1.8$ Ω, and $f = 1$ MHz. Carry out numerical simulations with the aid of MATLAB, during which the iterative points corresponding to each reference current are all started at $i_{\rm L} = 0$, $v_{\rm C} = 0$. After that, display the last 250 points after iterating 3000 points and the obtained bifurcation diagram using $I_{\rm ref}$ as bifurcation parameter is shown in Fig. 2.

It can be seen from Fig. 2 that when $I_{\rm ref}$ is small, the converter is working in period-1 orbit. As $I_{\rm ref}$ increases to 1.01 A, the period-doubling bifurcation occurs and the converter begins to work in period-2 orbit. With the continuous increase of $I_{\rm ref}$, period-2 orbit collides with border $I_{\rm b}$ when $I_{\rm ref}$ equals to 1.09 A, indicating the border collision bifurcation occurs. After that, the period-doubling bifurcation will not exist any longer, and the converter will fall into chaos via quasi-period-4 orbit. When $I_{\rm ref}$ adds up to 1.28 A or so, separate chaotic attractors combine together and the system falls into complete chaos eventually. In short, with the continuous increase of $I_{\rm ref}$, the converter will experience period-1 orbit, period-2 orbit, quasi-period-4 orbit and chaos successively.

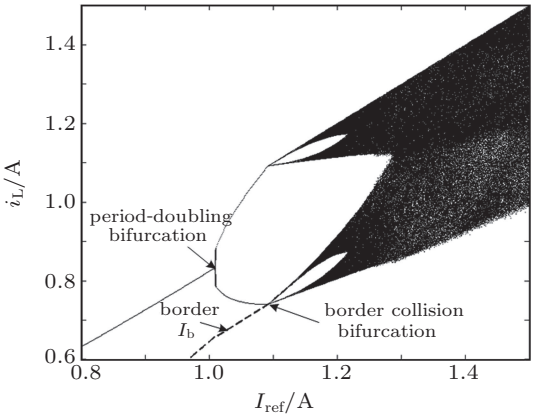


Fig. 2. Bifurcation diagram using $I_{\rm ref}$ as bifurcation parameter.

3.2. Typical time domain waveforms and phase portraits in $i_{\rm L}$–$v_{\rm C}$ plane

The peak current mode Buck converter circuit is constructed and simulated with PSIM, and the time domain waveforms as well as phase portraits in $i_{\rm L}$–$v_{\rm C}$ plane are plotted with the help of MATLAB depending on the simulation data. Figures 3(a)–3(d) present the time-domain waveforms of inductor current when $I_{\rm ref}$ equals to 1 A, 1.05 A, 1.12 A, and 1.3 A separately, and the corresponding phase portraits in $i_{\rm L}$–$v_{\rm C}$ plane are shown in Figs. 3(e)–3(h).

It can be seen from Fig. 3 that the working states of peak current mode Buck converter operating in period-1 orbit, period-2 orbit, quasi-period-4 orbit and chaotic state are consistent with the bifurcation diagram presented in Fig. 2.

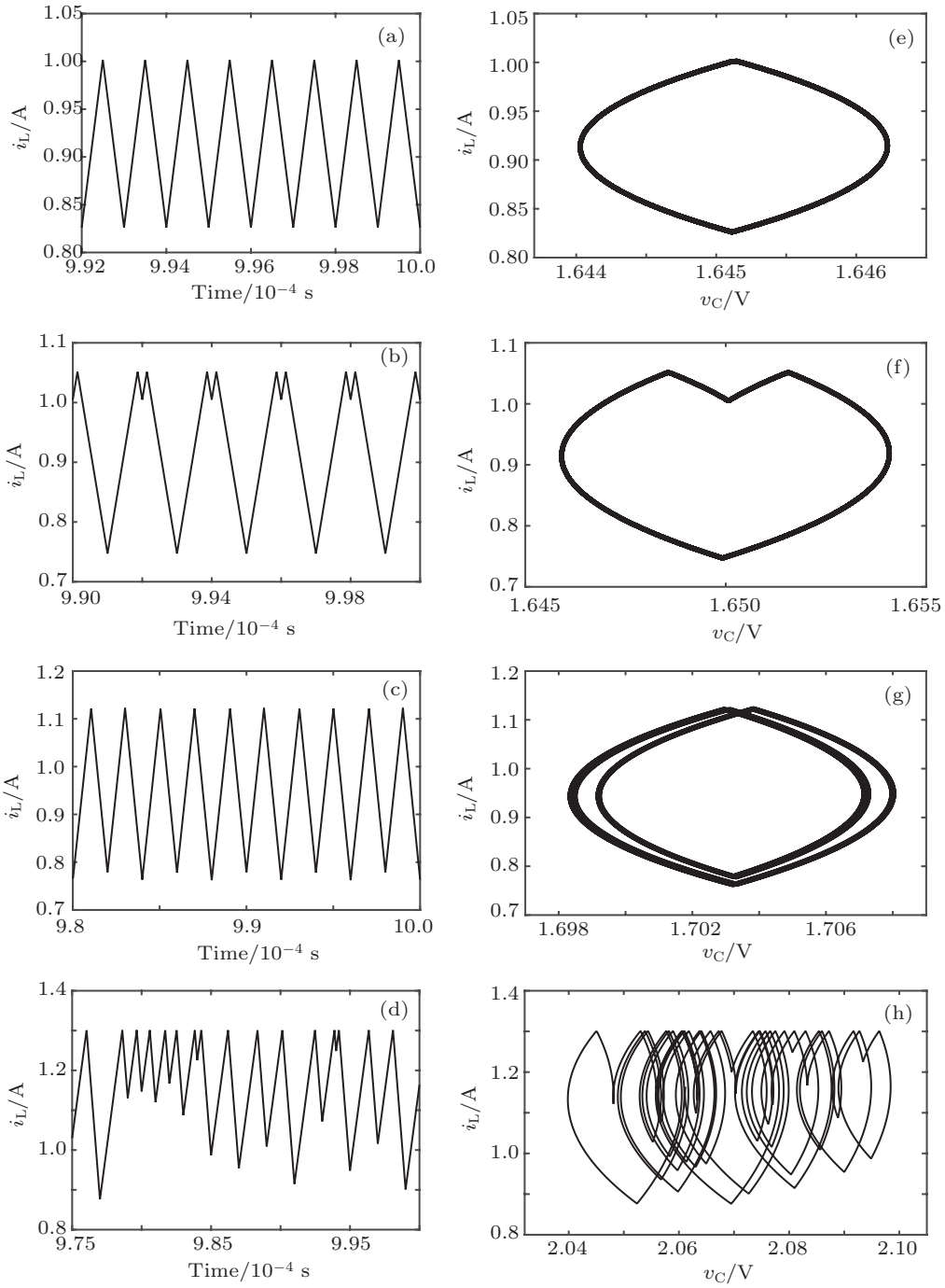


Fig. 3. Time-domain waveforms of inductor current ((a)–(d)) and phase portraits in i_L–v_C plane ((e)–(h)) at $I_{ref} = 1$ A ((a) and (e)), 1.05 A ((b) and (f)), 1.12 A ((c) and (g)), and 1.3 A ((d) and (h)).

3.3. The influence of switching frequency *f*

According to the discrete iterative mapping model (Eqs. (3)–(6)), there exist mutual restrictions between the switching frequency f and the other circuit parameters. That is, when the switching frequency of the converter is changed, the working state and stability of the system will be changed accordingly.

First, serve f as bifurcation parameter, whose range is from 0.2 MHz to 2.5 MHz. Next, set I_{ref} to 0.8 A, 1 A, and 1.2 A in sequence, and the obtained bifurcation diagrams using f as bifurcation parameter are shown in Figs. 4(a)–4(c) respectively.

From Fig. 4, it is found that when the reference current is relatively small ($I_{ref} = 0.8$ A), the inductor current i_L is always over border I_b in the whole variation range of f, indicating the converter is operating in stable period-1 orbit in this condition. When reference current increases to 1 A, as the switching frequency increases, the period-doubling bifurcation will occur, and after that the converter will enter period-2 orbit. When the reference current is large enough ($I_{ref} = 1.2$ A), with the increase of switching frequency f, the period-doubling bifurcation and the border collision bifurcation will occur successively, and the system will fall into chaos eventually.

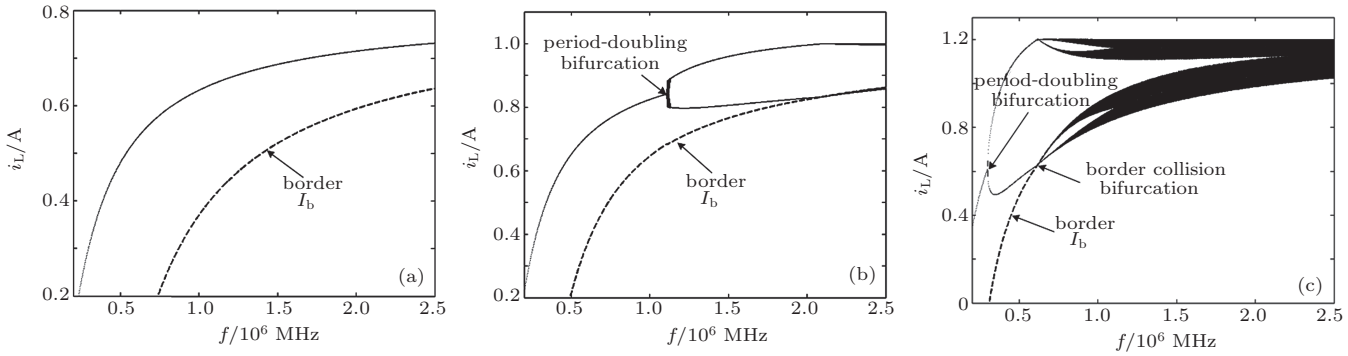


Fig. 4. Bifurcation diagrams using f as bifurcation parameter at $I_{\rm ref} = 0.8$ A (a), 1 A (b), and 1.2 A (c).

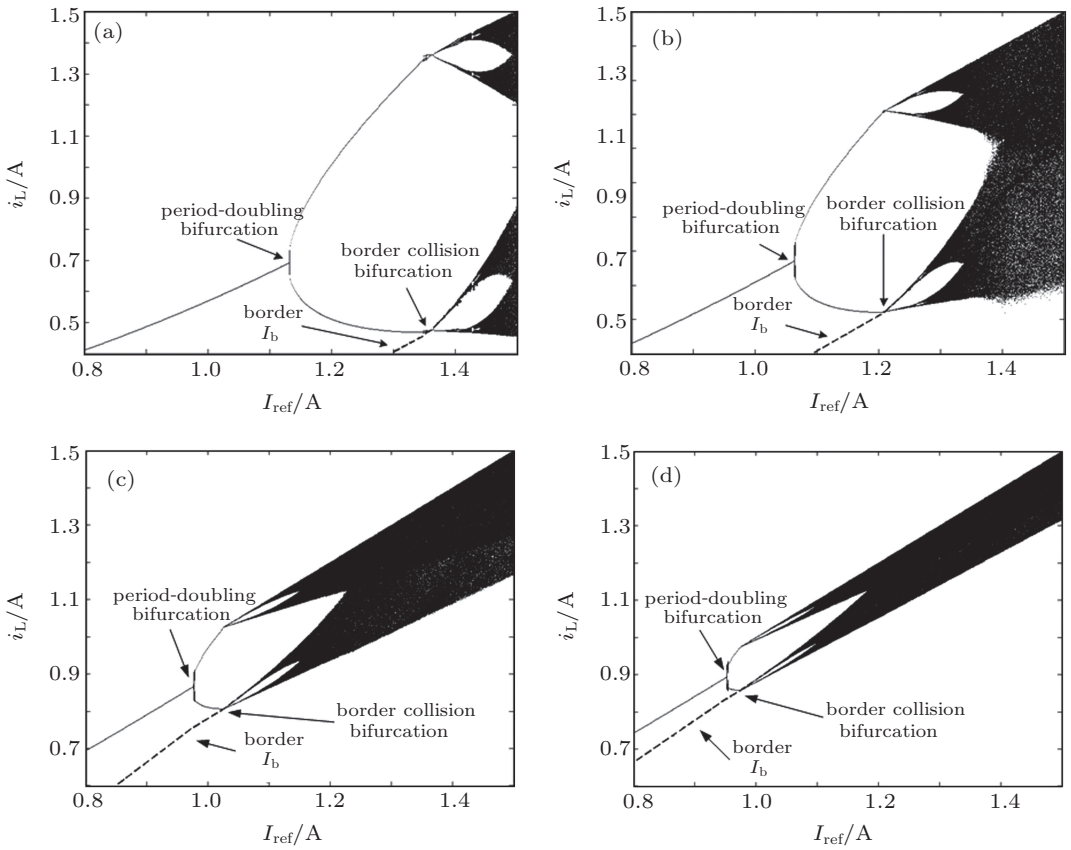


Fig. 5. Bifurcation diagrams using $I_{\rm ref}$ as bifurcation parameter at $f = 400$ kHz (a), 600 kHz (b), 1.6 MHz (c), and 3 MHz (d).

To sum up, with the increase of $I_{\rm ref}$, the corresponding switching frequency f is approaching to low-frequency stage continuously when period-doubling bifurcation happens, leading the converter to tend to be unstable. This trend can also be seen from Eq. (9) clearly.

Next, we are going to study the bifurcation diagrams of peak current mode Buck converter under different switching frequencies. Keeping the other circuit parameters unchanged, the bifurcation diagrams using $I_{\rm ref}$ as bifurcation parameter when f equals to 400 kHz, 600 kHz, 1.6 MHz, and 3 MHz are shown in Figs. 5(a)–5(d) respectively.

Combining Fig. 5 with Fig. 2, it can be found that with the increase of f, the corresponding $I_{\rm ref}$ decreases when the period-doubling bifurcation occurs, indicating the stable working range of the system becomes smaller. That is to say, switching frequency f and reference current $I_{\rm ref}$ are two inter-constraint parameters. However, the corresponding inductor current $i_{\rm L}$ increases when the period-doubling bifurcation occurs, representing greater load driving ability.

4. Stability analysis of peak current mode Buck converter through the Jacobian matrix

The stability of the system can be determined by computing the eigenvalues at the fixed point. Choosing circuit parameter φ (e.g., $I_{\rm ref}$ or f) as the bifurcation parameter, and the discrete iterative mapping model of the converter in CCM

(i.e., equations (5) and (6)) can be rewritten in the following equation:

$$\begin{bmatrix} i_{n+1} \\ v_{n+1} \end{bmatrix} = \begin{bmatrix} f_1(i_n, v_n, \varphi) \\ f_2(i_n, v_n, \varphi) \end{bmatrix}. \tag{11}$$

Let $i_{n+1} = i_n = i_Q$, $v_{n+1} = v_n = v_Q$, then the fixed point v_Q, i_Q can be obtained according to Eq. (11). The Jacobian matrix in the neighbourhood of the fixed point can be described as

$$\boldsymbol{J} = \left[\begin{array}{cc} \dfrac{\partial f_1}{\partial i_n} & \dfrac{\partial f_1}{\partial v_n} \\ \dfrac{\partial f_2}{\partial i_n} & \dfrac{\partial f_2}{\partial v_n} \end{array} \right] \Bigg|_{i_n = i_Q, v_n = v_Q}, \tag{12}$$

and its characteristic equation of the fixed point can be expressed as

$$\det(\lambda \boldsymbol{I} - \boldsymbol{J}) = 0. \tag{13}$$

The stability of the system is determined by the eigenvalues λ_1 and λ_2 at the fixed point. The corresponding φ when one of the eigenvalues equals to -1 is the parameter value at the period-doubling bifurcation point.[3,4,18] Using $I_{\rm ref}$ as bifurcation parameter while keeping the other parameters of the system unchanged, the obtained eigenvalues and system state are shown in Table 1.

As can be seen from Table 1, when $I_{\rm ref}$ increases to 1.0033 A, the period-doubling bifurcation occurs and the system switches from period-1 orbit to period-2 orbit. The analysis results and the bifurcation diagram in Fig. 2 are basically consistent.

Table 1. Eigenvalues and system state at different $I_{\rm ref}$ with $f = 1$ MHz.

$I_{\rm ref}$/A	Eigenvalue λ_1	Eigenvalue λ_2	State
0.8	–0.6436	0.9439	period-1 orbit
1.0	–0.9929	0.9461	period-1 orbit
1.002	–0.9972	0.9461	period-1 orbit
1.0033	–1.0000	0.9461	period-doubling bifurcation
1.01	–1.0148	0.9462	period-2 orbit

Next, by serving f as bifurcation diagram, the obtained eigenvalues and system state as $I_{\rm ref}$ equals to 0.8 A, 1 A, and 1.2 A are shown in Tables 2–4, respectively.

Table 2. Eigenvalues and system state at different f with $I_{\rm ref} = 0.8$ A.

f/MHz	Eigenvalue λ_1	Eigenvalue λ_2	State
1.0	–0.6436	0.9439	period-1 orbit
1.6	–0.6886	0.9652	period-1 orbit
2.25	–0.7119	0.9753	period-1 orbit
3.0	–0.7268	0.9815	period-1 orbit

Table 3. Eigenvalues and system state at different f with $I_{\rm ref} = 1$ A.

f/MHz	Eigenvalue λ_1	Eigenvalue λ_2	State
0.5	–0.8293	0.8923	period-1 orbit
1.0	–0.9929	0.9461	period-1 orbit
1.02	–0.9965	0.9471	period-1 orbit
1.05	–1.0017	0.9486	period-doubling bifurcation

Table 4. Eigenvalues and system state at different f with $I_{\rm ref} = 1.2$ A.

f/MHz	Eigenvalue λ_1	Eigenvalue λ_2	State
0.2	–0.7713	0.7422	period-1 orbit
0.28	–0.9632	0.8235	period-1 orbit
0.296	–0.9958	0.8336	period-1 orbit
0.3	–1.0037	0.8359	period-doubling bifurcation

It can be seen from Table 2 that when $I_{\rm ref}$ is relatively small ($I_{\rm ref} = 0.8$ A), the system is stable even when f reaches 3 MHz. According to Tables 3 and 4, as $I_{\rm ref}$ increases to 1 A and 1.2 A, the corresponding switching frequencies when the period doubling bifurcation occurs are about 1.05 MHz and 0.3 MHz respectively, which are consistent with the results presented in Fig. 4.

5. Experimental verification

In order to verify the correctness of previous theoretical analysis, an experimental circuit is built to test the nonlinear phenomena of the peak current mode Buck converter. The full schematic diagram and the photograph of the experimental circuit are shown in Figs. 6 and 7 respectively.

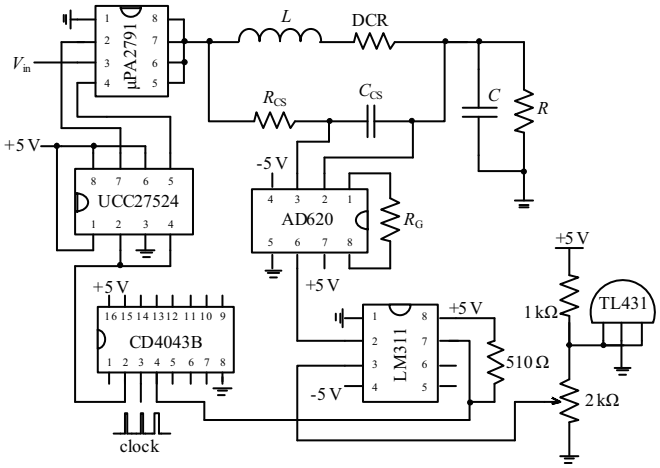


Fig. 6. Schematic diagram of the peak current mode Buck converter.

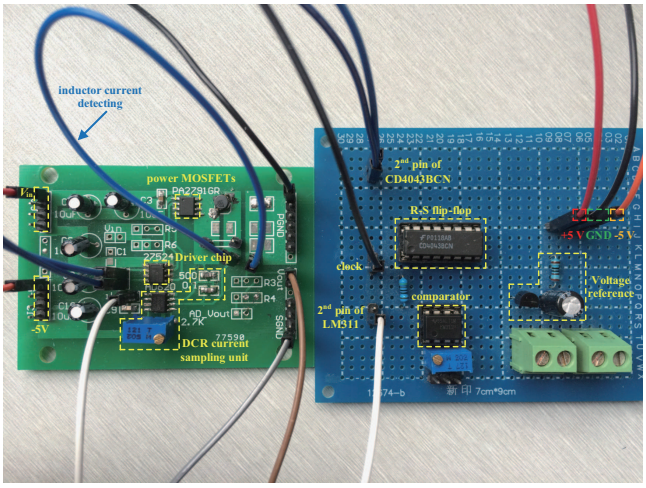


Fig. 7. (color online) Photograph of the experimental circuit.

In the main topology, the power tube is μPA2791 and the driver chip is UCC27524. The feedback path is mainly composed of current sampling circuit, an amplifier (AD620), a comparator (LM311) and an R-S flip-flop (CD4043BC). In this paper, we adopt DCR current sampling method[23] to obtain a voltage that is proportional to inductor current, and then the voltage is amplified by AD620, hence, the signal input into the inverting input port of the comparator is a reference voltage $V_{\rm ref}$ that is numerically equal to the reference current $I_{\rm ref}$.

The waveforms of inductor current and output voltage as well as phase portraits in $i_{\rm L}$–$V_{\rm o}$ plane at 1 MHz switching frequency when reference voltage $V_{\rm ref}$ is 0.95 V, 1.05 V, and 1.2 V are shown in Fig. 8.

As can be seen from Fig. 8, with the increase of $V_{\rm ref}$, the converter experiences the stable period-1 orbit, period-2 orbit and chaotic state successively, indicating the converter system tends to be unstable with the augment of $V_{\rm ref}$ at a certain switching frequency. The experimental results are consistent with previous analysis and simulation results.

Then we will verify the influence of switching frequency variation on system state. According to Figs. 8(c) and 8(f), when $f = 1$ MHz and $V_{\rm ref} = 1.2$ V, the peak current mode Buck converter is working in chaotic state. Keeping the reference voltage $V_{\rm ref} = 1.2$ V unchanged, the waveforms of inductor current and output voltage as well as phase portraits in $i_{\rm L}$–$V_{\rm o}$ plane with f equals to 600 kHz and 250 kHz are shown in Fig. 9.

Combining Figs. 8(c) and 8(f) with Fig. 9, it can be found that with the decrease of f, the converter experiences the chaotic state, period-2 orbit and stable period-1 orbit in sequence, namely the converter system is tending towards stability with the decrease of f at a certain reference voltage, which proved the experimental results are basically consistent with previous analysis and simulation results.

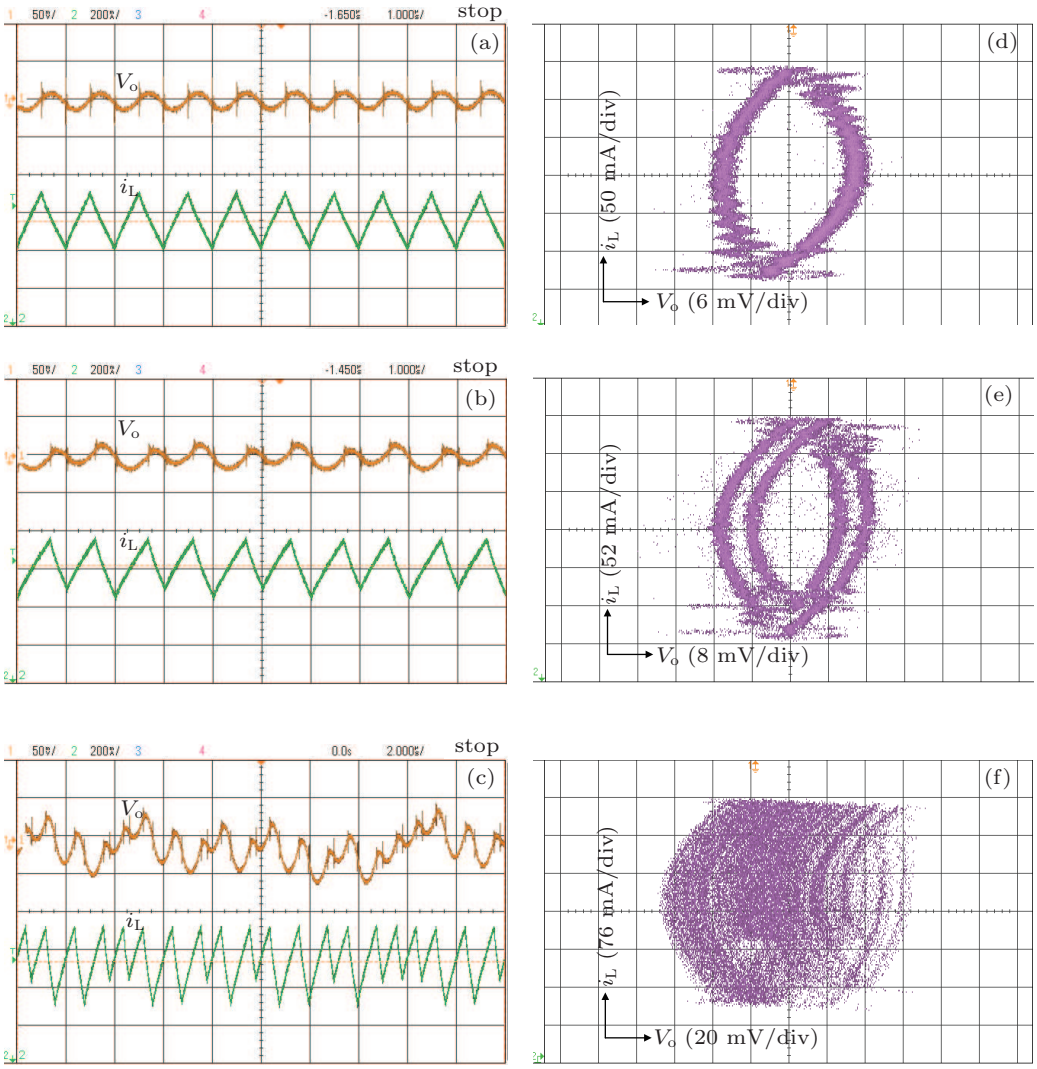


Fig. 8. (color online) Experimental waveforms of inductor current and output voltage ((a)–(c)) as well as phase portraits in $i_{\rm L}$–$V_{\rm o}$ plane ((d)–(f)) at $V_{\rm ref} = 0.95$ V ((a) and (d)), 1.05 V ((b) and (e)), 1.2 V ((c) and (f)) with $f = 1$ MHz.

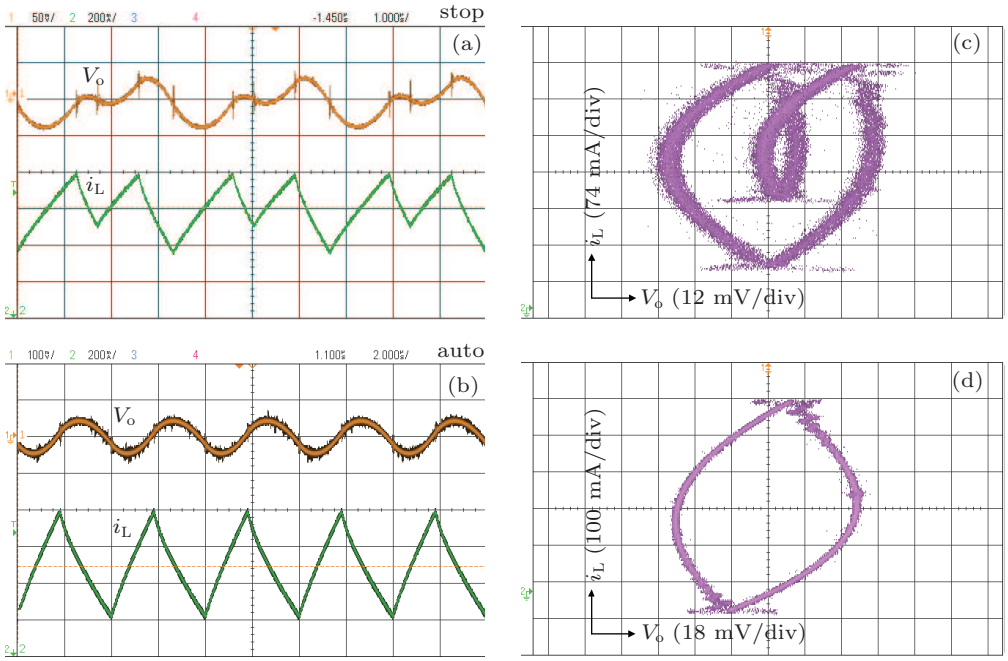


Fig. 9. (color online) Experimental waveforms of inductor current and output voltage as well as phase portraits in i_L–V_o plane at $f = 600$ kHz ((a) and (c)), 250 kHz ((b) and (d)) with $V_{ref} = 1.2$ V.

6. Conclusion

In this paper, the focus of our research is to study nonlinear phenomena in high frequency peak current mode Buck converter and to discover the relationship between switching frequency and system stability. First, we establish the two-dimensional discrete mapping model of the converter. After that, we derive the reference current at the period-doubling point and the border of inductor current. Next, the bifurcation diagrams are obtained through numerical simulation and plotted with the aid of MATLAB. Meanwhile, time domain waveforms and phase portrait in i_L–v_C plane are obtained through PSIM simulation, and are plotted with MATLAB on the basis of simulation data. Then, the Jacobian matrix is derived and the stability of the system is analyzed based on the eigenvalues of characteristic equations. Finally, to testify the validity of theoretical analysis, the experiment is carried out on a test circuit. Both the simulation and experimental results show that the converter tends to be unstable with the increase of reference current I_{ref}, as the corresponding switching frequency f is approaching to low-frequency stage continuously when the period-doubling bifurcation occurs. Moreover, with the increase of f, the stable working range of the system becomes smaller for the corresponding I_{ref} decreases when the period-doubling bifurcation occurs.

References

[1] Zhong S, Sha J, Xu J P, Xu L J and Zhou G H 2014 *Acta Phys. Sin.* **63** 198401 (in Chinese)
[2] Zhang X T, Ma X K and Zhang H 2008 *Acta Phys. Sin.* **57** 6174 (in Chinese)
[3] Zhou G H, Xu J P, Bao B C and Jin Y Y 2010 *Chin. Phys. B* **19** 060508
[4] Lai Y M, Tse C K and Chow M H L 2001 *Circ. Syst. Signal Pr.* **20** 695
[5] Wang F Q, Zhang H and Ma X K 2012 *Chin. Phys. B* **21** 020505
[6] Zhusubaliyev Z T, Soukhoterin E A and Mosekilde E 2003 *IEEE Trans. Circuits Syst. I* **50** 1047
[7] Zhusubaliyev Z T, Mosekilde E and Yanochkina O O 2011 *IEEE Trans. Power Electron.* **26** 1270
[8] Leng M R, Zhou G H, Zhang K T and Li Z H 2015 *Chin. Phys. B* **24** 100504
[9] Zou Y L, Luo X S and Chen G R 2006 *Chin. Phys.* **15** 1719
[10] Poddar G, Chakrabarty K and Banerjee S 1995 *IEEE Trans. Circuits Syst. I* **42** 502
[11] Yang Y W, Liu J L and Li B 2014 *Acta Phys. Sin.* **63** 040502 (in Chinese)
[12] Giaouris D, Banerjee S, Mandal K, Al-Hindawi M M, Abusorrah A, Al-Turki Y and El Aroudi A 2015 *Int. J. Bifur. Chaos* **25** 1550071
[13] Deane J H B 1992 *IEEE Trans. Circuits Syst. I* **39** 680
[14] Chan W C Y and Tse C K 1997 *IEEE Trans. Circuits Syst. I* **44** 1129
[15] Yang N N, Liu C X and Wu C J 2012 *Chin. Phys. B* **21** 080503
[16] Bao B C, Yang P, Ma Z H and Zhang X 2012 *Acta Phys. Sin.* **61** 220502 (in Chinese)
[17] Xu C D and Cheng K W E 2011 *IET Power Electron.* **4** 209
[18] Zhou G H, Xu J P and Bao B C 2010 *Acta Phys. Sin.* **59** 2272 (in Chinese)
[19] Xie F, Yang R and Zhang B 2010 *Acta Phys. Sin.* **59** 8393 (in Chinese)
[20] Xie F, Yang R and Zhang B 2011 *IEEE Trans. Circuits Syst. I* **58** 2269
[21] Hsieh F H, Wang H K, Chang P L and Syu S H 2013 *Proceedings of the 2013 International Conference on Machine Learning and Cybernetics*, July 14–17, 2013, Tianjin, China, p. 1796
[22] Bernardo M D and Vasca F 2000 *IEEE Trans. Circuits Syst. I* **47** 130
[23] Simon-Muela A, Petibon S, Alonso C and Chaptal J L 2008 *IEEE Trans. Ind. Electron.* **55** 3221